Mol Cell Biochem (2017) 426:205–213
DOI 10.1007/s11010-016-2893-9

Oxygen exchange and energy metabolism in erythrocytes of Rett syndrome and their relationships with respiratory alterations

Chiara Ciaccio[1] · Donato Di Pierro[1] · Diego Sbardella[1] · Grazia Raffaella Tundo[1] · Paolo Curatolo[2] · Cinzia Galasso[2] · Marta Elena Santarone[2] · Maurizio Casasco[3] · Paola Cozza[1] · Alessio Cortelazzo[4] · Marcello Rossi[5] · Claudio De Felice[6] · Joussef Hayek[7] · Massimo Coletta[1] · Stefano Marini[1]

Received: 3 October 2016 / Accepted: 2 December 2016 / Published online: 7 January 2017

Abstract Rett syndrome (RTT) is a neurodevelopmental disorder, mainly affecting females, which is associated to a mutation on the methyl-CpG-binding protein 2 gene. In the pathogenesis and progression of classic RTT, red blood cell (RBC) morphology has been shown to be an important biosensor for redox imbalance and chronic hypoxemia. Here we have evaluated the impact of oxidation and redox imbalance on several functional properties of RTT erythrocytes. In particular, we report for the first time a stopped-flow measurement of the kinetics of oxygen release by RBCs and the analysis of the intrinsic affinity of the hemoglobin (Hb). According to our experimental approach, RBCs from RTT patients do not show any intrinsic difference with respect to those from healthy controls neither in Hb's oxygen-binding affinity nor in O_2 exchange processes at 37 °C. Therefore, these factors do not contribute to the observed alteration of the respiratory function in RTT patients. Moreover, the energy metabolism of RBCs, from both RTT patients and controls, was evaluated by ion-pairing HPLC method and related to the level of malondialdehyde and to the oxidative radical scavenging capacity of red cells. Results have clearly confirmed significant alterations in antioxidant defense capability, adding important informations concerning the high-energy compound levels in RBCs of RTT subjects, underlying possible correlations with inflammatory tissue alterations.

Keywords Rett syndrome · Erythrocytes · Oxidative stress · Hemoglobin · Oxygen affinity · Energy metabolism

Abbreviations

RTT	Rett syndrome
RBC	Red blood cell
Hb	Hemoglobin
OS	Oxidative stress
NPBI	Plasmatic non-protein-bound iron
Met-Hb	Methemoglobin
CO-Hb	Carboxyhemoglobin
MDA	Malondialdehyde
ORAC	Reactive oxygen species scavenging capacity
ATP	Adenosine triphosphate
ADP	Adenosine diphosphate
AMP	Adenosine monophosphate
NAD^+	Nicotinamide adenine dinucleotide
NADPH	Nicotinamide adenine dinucleotide phosphate hydrogen
NADH	Nicotinamide adenine dinucleotide hydrogen

Chiara Ciaccio, Donato Di Pierro contributed equally to this work.

✉ Chiara Ciaccio
chiara.ciaccio@uniroma2.it

[1] Department of Clinical Sciences and Translational Medicine, University of Roma Tor Vergata, Via Montpellier 1, 00133 Rome, Italy

[2] Department of Systems Medicine, University Hospital of Rome Tor Vergata, Rome, Italy

[3] Federazione Medico Sportiva Italiana, Rome, Italy

[4] Department of Medical Biotechnologies, University of Siena, Siena, Italy

[5] Respiratory Pathophysiology and Rehabilitation Unit, University Hospital, AOUS, Siena, Italy

[6] Neonatal Intensive Care Unit, University Hospital, AOUS, Siena, Italy

[7] Child Neuropsychiatry Unit, University Hospital, AOUS, Siena, Italy

Introduction

Rett Syndrome (RTT; MIM312750) is the leading cause of a pervasive and complex neurodevelopmental disease in females. More than 95% of individuals with classic RTT carry sporadic *de novo* loss-of-function mutations in the X-linked methyl-CpG-binding protein 2 (*MECP2*) gene [1], which encodes a nuclear protein that binds methylated CpGs and regulates gene expression [2]. Other genes have been linked to additional rare variant RTT, including cyclin-dependent kinase-like 5 (*CDKL5*), forkhead box protein G1 (*FOXG1*), and the Netrin G1 genes [3, 4]. Although a wide variability in phenotypic severity is observed, in its classic form, RTT is characterized by a unique disease progression, beginning with an uneventful early infancy (6–18 months), followed by stagnation and regression of growth, motor, language, and social skills later in development [5, 6]. Notably, breathing disorders (i.e., chronic mild hypoxia with impaired lung gas exchange) are considered as a hallmark feature of the disease being among the key symptoms of RTT [7–10], and contributing to the developmental abnormalities in the brain and to a high rate of sudden and unexpected death [11]. It is widely recognized that the systemic oxidative stress (OS), triggered by associated hypoxia, acts as a primary driving force in the pathogenesis mechanism of classic RTT, this being supported by the evidence that OS biomarkers are related to the severity of neurological symptoms, mutation type, and clinical presentation [12, 13, 20]. The occurrence of a redox imbalance in RTT has been reported both in patients [12–16] and in experimental mouse models [17]. Notably, brain oxidative damage occurs already in the pre-symptomatic stage, as inferred by studies carried out in *Mecp2*-mutant murine models of Rett synrome [18–21].

Red blood cell (RBC) shape is abnormal in RTT and it appears to be mainly modulated by OS. In particular, leptocytes were found to be the predominantly altered erythrocyte shape in untreated typical RTT [22]. The percentages of abnormal RBCs shape were found to be related to an increased intraerythrocytic and plasmatic non-protein-bound iron (NPBI; i.e., free iron), and to the evidence of a membrane oxidative damage, as demonstrated by the increased formation of esterified F_2-IsoPs and 4-HNE Pas [22, 23]. In typical RTT patients, the evidences of OS damage in RBCs are strongly related to hypoxic conditions, as indicated by decreased SpO2 and PaO2 levels, coupled with increased methemoglobin (Met-Hb) and carboxyhemoglobin (CO-Hb) concentrations in RTT with respect to controls [20, 22]. Supplementation with ω-3 PUFAs has been shown to be able to partially rescue RBCs shape and to reduce clinical severity, improving pulmonary oxygen exchange and cardiopulmonary physiology [22]. Altogether, these findings suggest that monitoring of physiological properties of RBC as a function of OS damage can represent an important diagnostic and prognostic tool in this postnatal neurological disorder, in which the lung seems to represent an unexpectedly key organ for the disease pathogenesis and progression.

We have focused the present study on RBCs in order to evaluate the impact of oxidation and redox imbalance on several functional properties of this important biosensor. In particular, we have investigated for the first time in RTT patients the kinetics of oxygen release by RBCs and the intrinsic affinity of the hemoglobin (Hb) to possibly detect differences in the functional properties of RBCs related to oxygen exchanges and Hb affinity. Moreover, in order to identify alterations in antioxidant defense and metabolic process in RBCs from RTT, the energy metabolism of erythrocytes was analyzed by ion-pairing HPLC method and related to the levels of malondialdehyde (MDA), a marker of membrane lipid peroxidation [24], and to the reactive oxygen species scavenging capacity (ORAC assay).

Materials and methods

Subjects

A total of 15 female patients with clinical diagnosis of typical RTT (mean age: 11–15 years, range 2–21), as well as ten healthy female controls of comparable age free of any medication (mean age: 11–21 years, range 2–22), were enrolled in the study. RTT diagnosis and inclusion/exclusion criteria were based on the recently revised RTT nomenclature consensus. Blood samplings in the control group were carried out during routine health checks, always after informed consent while blood samplings in Rett patients were obtained during the periodic clinical checks. Institutional review board approval and informed consent from either the parents or the adult control subjects as well as the approval by the local ethical committee were obtained.

Blood sampling

Blood was collected in heparinized tubes and split into two aliquots; one was processed according to the HPLC analysis, the other was centrifuged at 3500 rpm for 5 min at 4 °C and the supernatant, containing plasma and buffy

coat, was removed. The erythrocyte pellet was washed three times and resuspended in isotonic buffer solution (58 mM NaP, 77.5 mM NaCl, 10 μM $CaCl_2$), with a final pH value of 7.4. Red blood cell suspension was then split and differently processed for kinetic analysis and oxygen-binding measurements.

Kinetics of oxygen release by RBCs

The kinetics of oxygen release by RBCs was carried out, within 1 h from withdrawal, by rapid mixing experiments using the SX18.MV stopped-flow apparatus (Applied Photophysics, Salisbury, UK) equipped with a diode array for spectra acquisition over 1 ms time range [25, 26]. Suspension of completely oxygenated red cells (in isotonic buffer solution, pH 7.4, 15 μM total heme concentration after mixing) was mixed with a deoxygenated isotonic solution containing 20 mmol L^{-1} sodium dithionite (Fluka Biochemika) at 37 °C.

Kinetic traces have been analyzed according to the following equation:

$$OD_{\text{obs}} = OD_0 \pm \sum_{i=1}^{i=r} DOD_i \cdot \exp(-{}^{i}k \cdot t)^n, \tag{1}$$

where OD_{obs} is the observed optical density at a selected wavelength and at a given time interval, OD_0 is the optical density at $t = 0$, r is the number of exponentials, DOD_i is the optical density change associated to the exponential i, ${}^{i}k$ is the rate constant of the exponential i, t is the time, and n is the Hill coefficient, as a phenomenological expression of the cooperativity of the kinetic process, accounting for the markedly autocatalytic O_2 release.

Equilibrium oxygen-binding measurements

Oxygen-binding measurements were obtained spectrophotometrically, at 37 °C, by tonometric method [27]. To determine its internal volume (i.e., V_{tot}) the tonometer was weighed before and after filling with distilled H_2O. Red blood cell suspensions (corresponding to about 15 μM total heme) were deoxygenated until deoxy-Hb was formed, as from the absorption spectra. Aliquots of air (ranging between 1 and 10 mL) were then injected into the tonometer by syringes; the oxygen pressure after each addition of air could be calculated according to the following relationship

$$pO_2(\text{mmHg}) = 152 \cdot \frac{V_{\text{ad}}}{V_{\text{res}}}, \tag{2}$$

where V_{ad} is the total volume of air added, V_{res} ($=V_{\text{tot}} - V_{\text{sample}}$) is the residual tonometer gas volume after RBC sample introduction, and 152 mmHg corresponds to the O_2 pressure at 1 atmosphere of air. After each addition, red cell suspension was incubated for 10 min at 37 °C, rotating the horizontally lying tonometer at 120 rpm around its axis; the absorbance change upon oxygenation was monitored by a Jasco-710 spectrophotometer (Tokyo, Japan) at 560 versus 577 nm. Oxygenation of the intraerythrocytic Hb was brought about in a step-wise manner so that each addition of O_2 would change the absorbance of the suspension by a given percentage (corresponding to the saturation degree Y) of the total absorbance change observed for complete oxygenation. Fractional saturation of Hb was determined from the absorbance changes, and the free oxygen concentration was calculated by subtracting the amount of bound oxygen from total oxygen present after each addition of air, as from Eq. (2). The cooperative nature of oxygen binding to Hb in RTT and controls was examined by Hill plot analysis, according to the following equation

$$Y = \frac{[HbO_2]}{[Hb] + [HbO_2]} = \frac{K_{\text{ov}} \cdot pO_2^n}{1 + K_{\text{ov}} \cdot pO_2^n}, \tag{3a}$$

where Y is percentage of oxygenated HbO_2, K_{ov} (mmHg^{-1}) is the overall oxygen-binding affinity, pO_2 is the oxygen pressure, and n is the Hill coefficient, expressing the cooperativity degree. A more appropriate and common way to represent O_2-binding isotherms is by the logarithmic plot, according to the following equation

$$\log\left(\frac{Y}{1-Y}\right) = \log(K_{\text{ov}}) + n \cdot \log(pO_2), \tag{3b}$$

Quantitative analysis of malondialdehyde and energy state

Peripheral venous blood samples were collected in heparinized tubes. After 10 min centrifugation at $1853 \times g$ and 4 °C, carried out within 2 min from withdrawal, erythrocytes were washed twice with a large volume of PBS. After the second wash, packed erythrocytes were gently resuspended with PBS to obtain a 5% hematocrit. 500 μL of this suspension was deproteinized by adding ice-cold 70% $HClO_4$ (20 μL). The suspension was centrifuged at $20{,}690 \times g$ for 10 min at 4 °C, neutralized by adding 5 μM K_2CO_3 (20 μL) in ice, filtered through a 0.45 μM Millipore-HV filter and then analyzed by HPLC (100 μL) for the simultaneous direct determination of MDA and adenine nucleotides [24, 28]. The employed HPLC assay for the energy state analysis offers the possibility to determine high-energy phosphate content without any chemical manipulation of samples, except for perchloric acid deproteinization in order (i) to minimize the risk of modifications in the pattern of metabolites by proteins and (ii)

to avoid any possible HPLC analytical column obstruction caused by proteins [29, 30]. Concentrations of high-energy phosphates were determined on 100 μL of perchloric acid extract by an ion-pairing HPLC method [29–31] using a Kromasil 250 × 4.6 mm, 5 μm particle size column, with its own guard column (Eka Chemicals AB, Bohus, Sweden), and using tetrabutylammonium hydroxide as the pairing reagent. Briefly, the separation of different metabolites was obtained by forming a step gradient (adapted to the column length increase compared to the original method) [30] with two buffers of the following composition: buffer A, 10 mM tetrabutylammonium hydroxide, 10 mM KH_2PO_4, 0.25% methanol pH 7.00; buffer B, 2.8 mM tetrabutylammonium hydroxide, 100 mM KH_2PO_4, 30% methanol pH 5.50. The gradient was: 10 min 100% buffer A; 3 min 90% buffer A; 10 min 70% buffer A; 12 min 55% buffer A; 15 min 45% buffer A; 10 min 25% buffer A; 5 min 0% buffer A. The flow rate throughout the chromatographic runs was 1.2 mL/min and the column temperature was kept at a constant 23 °C using water-jacketed glassware. The HPLC apparatus consisted of a Surveyor LC Pump (ThermoFinnigan Italia, Rodano, Milan, Italy) connected to a Surveyor PDA Detector (ThermoFinnigan Italia) at 200–300 nm. Acquisition and analysis of data were performed using the ChromQuest program (ThermoQuest Italy). Comparison of areas, retention times, and absorbance spectra of the peaks of sample chromatograms with those of freshly prepared ultrapure standards made it possible to identify and calculate the concentration of the different metabolites. Both Hb and percentage haemolysis were calculated by standard hematological techniques [30], using a Jasco-685 double beam spectrophotometer. Same chromatograms also allowed us to identify and calculate MDA concentrations. ATP/ADP and ATP/AMP ratios, as well as NAD^+ content (μM) were used to identify intracellular energy content.

Oxygen radical absorbance capacity (ORAC) assay

The ORAC assay is based on the dose- and time-dependent decrease in the fluorescence intensity of β-phycoerythrin (β-PE) (Sigma-Aldrich Co, St. Louis, MO) when oxidized by oxygen radicals [32]. It measures the antioxidant capacity of a substance in terms of its ability to inhibit or delay β-PE peroxidation. AAPH [2.2′-Azobis(2-amino-propane) dihydrochloride], purchased from Polyscience (Warrington, PA), was used as the free-radical generator. Briefly, 20 μL of fresh whole blood was diluted in 10 mL of 75 mM phosphate buffer pH 7.0. After centrifugation to remove RBC ghosts, 100 mL of supernatant was used to evaluate redox scavenging activity. The final reaction mixture (2 mL) contained 1750 mL of 75 mM phosphate buffer (pH 7.0) and 100 μL of β-PE (1 mg dissolved in 88.2 mL of 75 mM phosphate buffer pH 7). A total of 0.1 mL of 20 μM Trolox (6-hydroxy-2,5,7,8-tetramethyl-2-carboxylic acid) in 75 mM phosphate buffer pH 7, buffer alone (blank), or hemolysed blood were added. After 15 min at 37 °C, 50 μL of 160 mM AAPH in a phosphate buffer was added. Beta-PE fluorescence was measured with a Varian Cary Eclipse Fluorescence Spectrofotometer (Varian Ltd., Madrid, Spain) at $\lambda = 546$ nm (λ excitation) and $\lambda = 573$ nm (λ emission). Measurements were made every 2.5 min at 37 °C for 1 h or until the fluorescence variation dropped below 2%. The ORAC of the sample was expressed as Micromol Trolox Equivalents/g and calculated as $[(As-Ab)/(At-Ab)]ka$, where As is the area under the curve (AUC) of β-PE in the sample, calculated with the Origin 2.8 Integration Program (MicroCal Software, LLC, Northhampton, MA), At is the AUC of the Trolox, Ab is the AUC of the control, k is the dilution factor (1:500 for the blood), and a is the concentration of the Trolox in mmol L^{-1}.

Statistical analysis

All samples were run on HPLC twice, and ORAC was performed in triplicate. Results are given as an average among patients ±SD. Data were entered into the GraphPad Prism statistical analysis program (GraphPad, San Diego). Comparison of results was performed by one-way analysis of variance (ANOVA). Bonferroni's test was used for multiple comparisons and Tukey's test was used to analyze media and standard deviations in different experiments. Differences between groups were considered statistically significant when $p < 0.05$.

Results and discussion

It is widely recognized that RTT may arise from systemic physiological abnormalities including OS [12–14, 20], mitochondrial abnormalities [33, 34], and immune dysregulation/inflammation [35, 36], rather than being a purely central nervous system disorder. In particular, the oxidative hypothesis is able to explain several features of this syndrome (e.g., its genotype–phenotype correlation and clinical heterogeneity), being supported by the evidence that OS biomarkers are related to neurological symptoms severity, mutation type, and clinical presentation [37, 38]. The erythrocyte seems to be one of the most important tools of antioxidant defenses in the whole body [39]. If the oxidative insult of the microenvironment overcomes the RBCs' defenses, this cell undergoes oxidative alterations, such as change of rheologic/functional properties [22]. It is conceivable that, in the presence of an intense and chronic OS, it is not possible to fully repair the damage [39]. In RBC of

RTT patients oxidants induce an altered RBC shapes (i.e., leptocytes) and increased iron release in a free redox active form (NPBI, i.e., non-protein-bound iron), together with an increased level of erythrocyte membrane esterification of F_2-IsoPs and 4-HNE Pas [22, 23, 40]. Interestingly, despite the oxidative damage to the RBC membrane, no pits and holes, usually associated with lipid peroxidation, were observed in the erythrocytes from RTT patients [22, 39] and, correspondingly, on the clinical side, no hemolytic anemia is commonly observed in RTT patients [22].

Moreover, no significant difference was observed in the RBC antioxidant enzyme activities (i.e., glutathione peroxidase, glutathione reductase, and catalase activities) between RTT patients and the control group, whereas erythrocyte superoxide dismutase activities were significantly decreased in Rett subjects as compared with controls [41].

In typical RTT patients, a hypoxic condition is evidenced [42–44], and it is associated with the abnormal erythrocyte shapes and with an increase in Met-Hb and CO-Hb concentrations in comparison to controls, coupled with a decrease in peripheral and arterial O_2 levels [22, 23]. These alterations were more prominent when associated to an enhancement of iron release and lipid peroxidation, preventable by ω-3 PUFAs [22]. Overall, these findings suggest that, in this particular form of postnatal neurological syndrome, in which breathing disorders and the related levels of oxidative damage in erythrocytes and plasma significantly contribute to the progression of the disease, red blood cell can represent a valuable cell target model for monitoring the degree of phenotype severity. Our study was aimed to investigate, in RTT patients, the impact of oxidation and redox imbalance on several functional properties of RBCs, never deeply investigated before. The kinetics of oxygen release by RBCs and the intrinsic affinity of the intraerythrocytic Hb have been investigated for the first time in RTT subjects to possibly detect differences in the functional properties of RBCs, related to oxygen exchange and Hb affinity.

The kinetics of oxygen release has been followed by the stopped-flow and analyzed according to Eq. (1) [26, 27].

Table 1 Kinetics of oxygen release by RBCs and Hb oxygen affinity determination

	k (s^{-1})	K_{ov} ($mmHg^{-1}$)	n
Rett syndrome ($n = 15$)	200 ± 22	0.051 ± 0.015	1.98 ± 0.21
Controls ($n = 10$)	212 ± 28	0.047 ± 0.018	1.82 ± 0.18

Rate of O_2 release (k), oxygen affinities (K_{ov}), and Hill's coefficient (n) at pH 7.4 and 37 °C from red cells in RTT and healthy controls matching for age and gender. k values were calculated according to Eq. (1); K_{ov} and n data were obtained according to Eq. (3b). Each value represents the mean of samples ±SD

Data are reported in Table 1 together with those of Hb oxygen affinity (K_{ov} values) and cooperativity (Hill's coefficient, n), which were analyzed according to Eq. (3b). The reported values of n refer to those obtained by equilibrium oxygen affinity, since they are more readily compared with literature data. According to this experimental approach, it appears evident that RBCs from RTT patients and those from healthy controls display closely similar parameters both for Hb O_2 affinity and rate of O_2 release at 37 °C. This becomes evident also by comparing two typical O_2 release kinetic processes by RTT patients and controls (Fig. 1a) and two typical O_2-binding isotherms (Fig. 1b).

RBCs show a characteristic biconcave shape, which is of key importance for all their functions (i.e., deformability and O_2 exchange), but it also very susceptible to morphological changes with consequent lack of functionality. Changes in osmolarity, pH conditions, and presence of oxidants are reported among the factors inducing

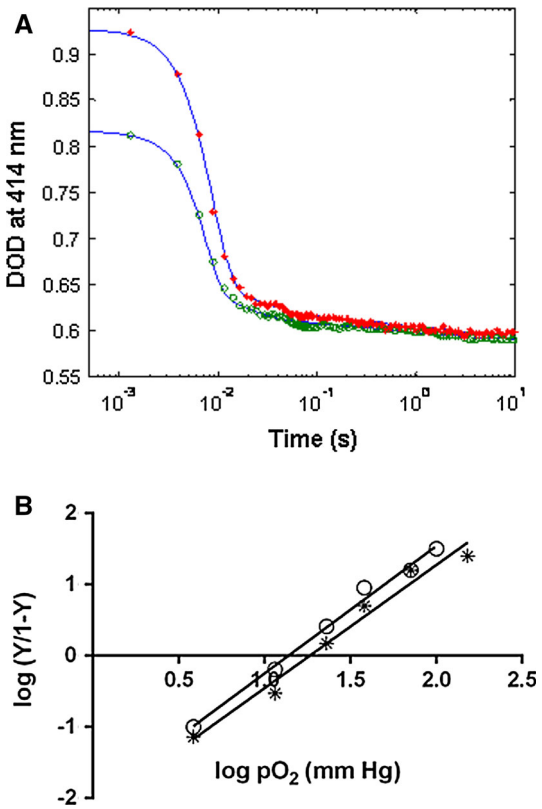

Fig. 1 **a** Time courses for the release of O_2 from red blood cells. Kinetic traces, at pH 7.4 and 37 °C at $\lambda = 414$ nm, for RTT erythrocytes (*asterisk symbol*) and healthy controls (*open circle*). Continuous lines correspond to the non-linear least squares fitting of data according to Eq. (1). **b** Hill plots of oxygen-binding curves of Hb. Oxygen-binding isotherms are shown, at pH 7.4 and 37 °C, for RTT erythrocytes (*asterisk symbol*) and healthy controls (*open circle*). Continuous lines correspond to the non-linear least squares fitting of data according to Eq. (3b)

Table 2 Erythrocyte energy metabolism, lipid peroxidation (MDA), and ORAC assay results

	MDA	ORAC	NAD	AMP	ADP	ATP	ATP/ADP	ATP/AMP
Reet syndrome ($n = 15$)	0.32 (0.07)	2.61 (0.29)	637 (97)	39.5 (2.7)	696 (39.2)	1266 (114)	1.85 (0.3)	32 (4.3)
Controls ($n = 10$)	0.035 (0.015)	4.29 (0.71)	401 (27)	29.7 (5.7)	349.2 (52.3)	1822.7 (168)	5.2 (1.3)	60.7 (18)
Variation (%) versus Controls	814%	−39%	59%	33%	99%	−31%	−64%	−47%

Determination of high-energy phosphates was carried by HPLC on 100 µL of neutralized perchloric acid extracts of erythrocytes suspension at a 5% hematocrit. NAD values are considered as the total nicotinic coenzyme pools (NADH + NAD^+). Each value represents the mean (SD) of samples. MDA and metabolites are expressed as µmol L^{-1} and ORAC values are expressed as mM Trolox equivalent

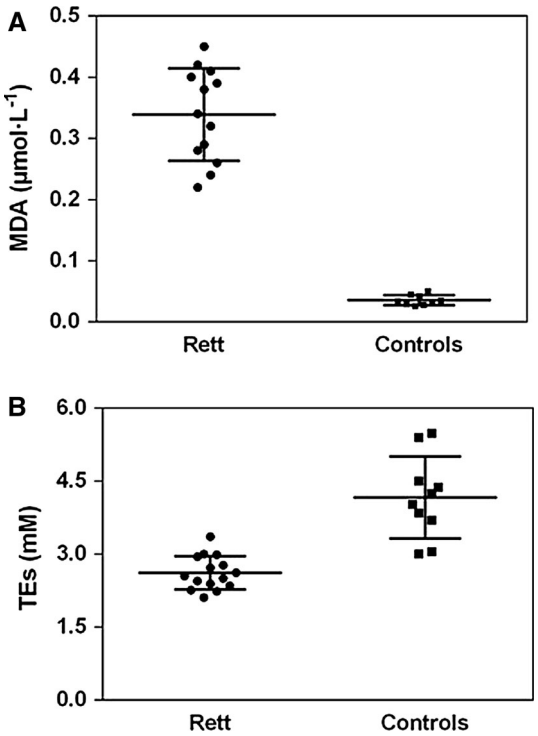

Fig. 2 Levels of lipid peroxidation (MDA) (**a**) and oxygen radical absorbance capacity (ORAC assay) (**b**). The ORAC values are expressed as mM Trolox equivalent (TEs). *Lines* indicate mean with SD and *symbols* correspond to individual data points from patients with Rett syndrome ($n = 13$) and controls ($n = 10$)

morphological modifications and changes in rheological properties of RBCs [23, 45–47]. Thus, although the oxygen release depends markedly on the surface area/volume ratio and internal environment of the cell, as a result of our data, the in vitro dynamic of oxygen release by RBCs doesn't seem to be compromised by the severe alteration of morphology observed in RTT erythrocytes [22]. Furthermore, our results show that the oxygen affinity and the cooperative nature of oxygen binding, determined spectrophotometrically for Hb of patients, were in every respect similar to those obtained for controls (Table 1; Fig. 1b). Even though this information concerns only the intrinsic functional properties of Hb and eventual alterations in the intraerythrocytic metabolites and allosteric modulators which affect the affinity of the Hb (i.e., pH, carbon dioxide, adenosine triphosphate or 2,3-bisphosphoglycerate) [48, 49], we can roughly postulate that the highly prooxidant environment of the erythrocyte in RTT (i.e., increased NPBI, alteration in Met-Hb and CO-Hb concentrations) doesn't seem to have a role in affecting the Hb oxygenation properties. Anyhow, it must be stressed that this experimental approach is able to detect only functional alterations related to the role of Hb as O_2 carrier. Therefore, functional modifications due to shape abnormalities or altered rheological properties of the RTT erythrocytes "in vivo" might not be detected, since the experimental conditions do not reproduce what actually occurs in the lung and/or in the system capillaries, where RBCs are squeezed and O_2 release takes place under grossly shape deforming conditions, which eventually magnify membrane elasticity alterations.

Therefore, the close functional similarity between RTT erythrocytes and those from healthy controls simply rules out that the gas exchange alterations, previously reported [22], could be referred to a modified intrinsic O_2 transport function of RTT RBCs. On the other hand, it also comes out in a clearcut fashion that respiratory alterations do not stem from a reduced capability of O_2 transport for RBCs from RTT patients, as indicated by the closely similar O_2 affinity and cooperativity (see Table 1).

A further aspect reviewed in our study concerned the antioxidant defense capability and the energy metabolism in RBCs from RTT. Detection of the main substances of energy metabolism (i.e., ATP, AMP and NAD^+) on cell extracts has been undertaken by employing the HPLC ion-pairing method and it has been related to the MDA levels and ORAC values. As expected, data clearly envisage a severe OS condition in erythrocytes from RTT patients (see Table 2; Fig. 2). In particular, an increased level of MDA (up to tenfold) was observed in RTT patients together with a significant reduced antioxidant defense capability (ORAC −39.2%) (Table 2; Fig. 2a, b respectively). As reported in Table 2, the levels of the high-energy phosphorylated compounds were significantly altered in RTT red cells. In particular, a relevant depletion of ATP was observed, as indicated by a concentration of $\approx$1823 µmol L^{-1} in controls and $\approx$1266 µmol L^{-1} in RTT erythrocytes. A concomitant increase of ADP and

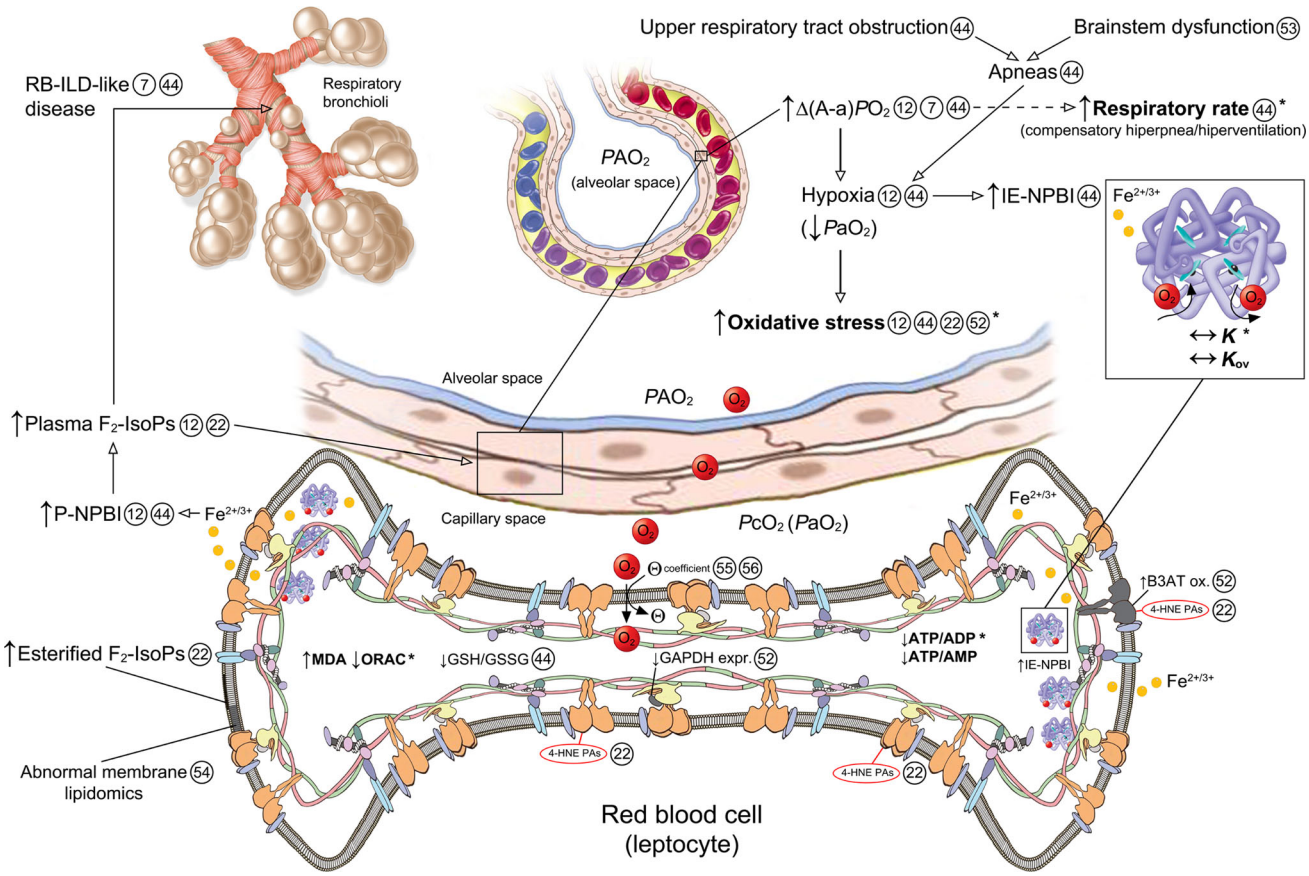

Fig. 3 Hypothetical diagram of respiratory pathophysiology in typical Rett Syndrome. ↑ increase; ↓ decrease; ↔ unchanged; *RB-ILD* respiratory bronchiolitis-interstitial lung disease; *Δ(A-a)PO*$_2$ oxygen alveolar–arterial gradient; *F*$_2$*-IsoPs* F$_2$- Isoprostanes; *IE-NPBI* intra-erythrocyte non-protein-bound iron; *P-NPBI* plasma non-protein-bound iron; *GSSG* glutathione oxidized form; *GSH* glutathione reduced form; *4-HNE Pas* 4-hydroxynonenal protein adducts; *MDA* malondialdehyde; *Fe*$^{2+/3+}$ redox free iron; *GAPDH* glyceraldehyde-3-phosphate dehydrogenase; *expr.* expression; *B3AT* band 3 anion transport protein; *ox.* oxidation; *ATP* adenosine triphosphate; *ADP* adenosine diphosphate; *AMP* adenosine monophosphate; *PAO*$_2$ partial alveolar pressure of oxygen; *PaO*$_2$ partial arterial pressure of oxygen; *PcO*$_2$ *(PaO*$_2$*)* partial capillary pressure of oxygen; *K* rate of oxygen release; *K*$_{ov}$ oxygen affinities; *ORAC* reactive oxygen species scavenging capacity; *Θ* oxygen diffusion coefficient; *Present work

AMP (up 99 and 33%, respectively) was detected with a resulting decrease of ATP/ADP and ATP/AMP ratios (−64 and −47%, respectively). In addition, an increase (up to 59%) of the NAD values, considered as the total nicotinic coenzyme pools (NAD^+ + NADH), were observed in RTT red cells. Most of the energy is used in erythrocytes to protect iron and other cytoplasmic and membrane molecules from oxidation through either scavenging of redox reactive species and/or reduction of the already oxidized molecules. In RBCs, where neither mitochondria nor nuclei are present, the level of high-energy compounds is strictly modulated and directly linked to the redox state of erythrocytes, such that an increase in redox-protective response depletes the RBCs from high-energy compounds, like NADPH (GSH/GSSG regulator), NADH (cofactor in the Met-Hb reductase reaction), and ATP [29, 30, 50]. Therefore, determination of high-energy phosphate nucleotides (i.e., ATP/ADP, ATP/AMP ratios), reflecting changes in cell energy state, can provide information about the intracellular redox state of RBCs. On the other hand, it worth outlining that the extent of ATP decrease does not affect significantly the O_2 affinity of intraerythrocytic Hb [51].

In Fig. 3 we sketch the complexity of factors influencing the respiratory mechanism, underlining alterations exhibited by RTT patients. It is quite obvious that the whole regulatory process is very complex and certainly the gas exchange abnormality observed in RTT patients cannot be the result of a single alleged mechanism, but it is rather the result of several contributing factors, involving OS and chronic subclinical inflammation in which terminal bronchioles and alveoli are likely a major inflammatory target of the disease [44].

Therefore, on the basis of the present study, we can hypothesize that the dynamics of the oxygen exchanges of erythrocytes with the environment and the intrinsic O_2

transport function of RTT RBCs is normal and that the observed pulmonary gas exchange impairment in RTT patients should be rather attributed to some inflammatory alteration which affects O_2 diffusion in the lungs, possibly at the level of terminal bronchioles and alveoli. In this perspective, such hypothesis could underline a connection between the redox imbalance, indeed detected in RBCs, and the inflammation-linked histological and functional alterations of tissues in the pulmonary system, bringing about the respiratory syndrome.

In conclusion, from this investigation on RBCs from RTT the "OS hypothesis" emerges as a systemic metabolic alteration, likely spread over to all body districts of RTT patients, and the respiratory alteration appears only as a consequence of this dismetabolism in pulmonary tissues without any consequence on the blood gas transport function.

In any case, our findings strengthen the importance of RBCs as a suitable biological tool for detecting markers of oxidative damage in RTT and underline the link between the biochemistry of OS and the pathogenesis of the disease.

Acknowledgements This work has been partially supported by the Federazione Medicina Sportiva Italiana (FMSI) and Associazione ProRett Siena.

References

1. Amir RE, Van den Veyver IB, Wan M, Tran CQ, Francke U et al (1999) Rett syndrome is caused by mutations in X-linked MECP2, encoding methyl-CpG-binding protein 2. Nat Genet 23:185–188
2. Chahrour M, Jung SY, Shaw C, Zhou X, Wong ST et al (2008) MeCP2, a key contributor to neurological disease, activates and represses transcription. Science 320:1224–1229
3. Mari F, Azimonti S, Bertani I, Bolognese F, Colombo E et al (2005) CDKL5 belongs to the same molecular pathway of MeCP2 and it is responsible for the early-onset seizure variant of Rett syndrome. Hum Mol Genet 14:1935–1946
4. Ariani F, Hayek G, Rondinella D, Artuso R, Mencarelli MA et al (2008) FOXG1 is responsible for the congenital variant of Rett syndrome. Am J Hum Genet 83:89–93
5. Glaze DG (2005) Neurophysiology of Rett syndrome. J Child Neurol 20:740–746
6. Chahrour M, Zoghbi HY (2007) The Story of Rett Syndrome: from clinic to neurobiology. Neuron 56:422–437
7. De Felice C, Guazzi G, Rossi M, Ciccoli L, Signorini C et al (2010) Unrecognized lung disease in classic Rett syndrome: a physiologic and high-resolution CT imaging study. Chest 138:386–392
8. Johnson CM, Cui N, Zhong W, Oginsky MF, Jiang C (2015) Breathing abnormalities in a female mouse model of Rett syndrome. J Physiol Sci 65:451–459
9. Katz DM, Dutschmann M, Ramirez JM, Hilaire G (2009) Breathing disorders in Rett syndrome: progressive neurochemical dysfunction in the respiratory network after birth. Respir Physiol Neurobiol 168:101–108
10. Ramirez JM, Ward CS, Neul JL (2013) Breathing challenges in Rett syndrome: lessons learned from humans and animal models. Respir Physiol Neurobiol 189:280–287
11. Kerr AM, Armstrong DD, Prescott RJ, Doyle D, Kearney DL (1997) Rett syndrome: analysis of deaths in the British survey. Eur Child Adolesc Psychiatry 6(Suppl 1):71–74
12. De Felice C, Ciccoli L, Leoncini S, Signorini C, Rossi M et al (2009) Systemic oxidative stress in classic Rett syndrome. Free Radic Biol Med 47:440–448
13. Pecorelli A, Ciccoli L, Signorini C, Leoncini S, Giardini A et al (2011) Increased levels of 4HNE-protein plasma adducts in Rett syndrome. Clin Biochem 44:368–371
14. Hamburger A, Gillberg C, Palm A, Hagberg B (1992) Elevated CSF glutamate in Rett syndrome. Neuropediatrics 23:212–213
15. Leoncini S, De Felice C, Signorini C, Pecorelli A, Durand T et al (2011) Oxidative stress in Rett syndrome: natural history, genotype, and variants. Redox Rep 16:145–153
16. Signorini C, Leoncini S, De Felice C, Pecorelli A, Meloni I, et al. (2014) Redox imbalance and morphological changes in skin fibroblasts in typical Rett syndrome. Oxid Med Cell Longev. p. 195935
17. Grosser E, Hirt U, Janc OA, Menzfeld C, Fischer M et al (2012) Oxidative burden and mitochondrial dysfunction in a mouse model of Rett syndrome. Neurobiol Dis 48:102–114
18. Robinson L, Guy J, McKay L, Brockett E, Spike RC et al (2012) Morphological and functional reversal of phenotypes in a mouse model of Rett syndrome. Brain 135:2699–2710
19. Guy J, Gan J, Selfridge J, Cobb S, Bird A (2007) Reversal of neurological defects in a mouse model of Rett syndrome. Science 315:1143–1147
20. De Felice C, Della Ragione F, Signorini C, Leoncini S, Pecorelli A et al (2014) Oxidative brain damage in Mecp2-mutant murine models of Rett syndrome. Neurobiol Dis 68:66–77
21. Tropea D, Giacometti E, Wilson NR, Beard C, McCurry C et al (2009) Partial reversal of Rett syndrome-like symptoms in MeCP2 mutant mice. Proc Natl Acad Sci USA 106:2029–2034
22. Ciccoli L, De Felice C, Paccagnini E, Leoncini S, Pecorelli A et al (2012) Morphological changes and oxidative damage in Rett Syndrome erythrocytes. Biochim Biophys Acta 1820:511–520
23. Ciccoli L, De Felice C, Leoncini S, Signorini C, Cortelazzo A et al (2015) Red blood cells in Rett syndrome: oxidative stress, morphological changes and altered membrane organization. Biol Chem 396:1233–1240
24. Di Pierro D, Tavazzi B, Lazzarino G, Giardina B (1992) Malondialdehyde is a biochemical marker of peroxidative damage in the isolated repurfesed rat heart. Mol Cell Biochem 116:193–196
25. Coletta M, Giardina B, Amiconi G, Gualtieri P, Benedetti PA et al (1985) Kinetics of the reaction of intraerythrocytic haemoglobin by single cell microspectroscopy: effect of shape and osmolarity. FEBS Lett 190:217–220
26. Vandegriff KD, Olson JS (1984) The kinetics of O_2 release by human red blood cells in the presence of external sodium dithionite. J Biol Chem 259(20):12609–12618
27. Giardina B, Amiconi G (1981) Measurement of binding of gaseous and nongaseous ligands to hemoglobins by conventional spectrophotometric procedures. Meth Enzymol 76:417–427
28. Lazzarino G, Di Pierro D, Tavazzi B, Cerroni L, Giardina B (1991) Simultaneous separation of malondialdehyde, ascorbic acid and adenite nucleotide derivatives from biological samples by ion pairing high- performance liquid chromatography. Anal Biochem 197:191–196
29. Tavazzi B, Di Pierro D, Amorini AM, Fazzina G, Tuttobene M et al (2000) Energy metabolism and lipid peroxidation of human erythrocytes as a function of increased oxidative stress. Eur J Biochem 267:684–689
30. Tavazzi B, Amorini AM, Fazzina G, Di Pierro D, Tuttobene M et al (2001) Oxidative stress induces impairment of human erythrocyte energy metabolism through the oxygen radical-mediated

direct activation of AMP-deaminase. J Biol Chem 276:48083–48092
31. Di Pierro D, Tavazzi B, Perno CP, Bartolini M, Balestra E et al (1995) An ion pairing high performance liquid chromatography method for the simulateneous determination of nucleotides, deoxynucleotides, nicotinic coenzymes, oxypurines, nucleosides and bases. Anal Biochem 231:407–412
32. Cao G, Alessio HM, Cutler RG (1993) Oxygen-radical absorbance capacity assay for antioxidants. Free Radic Biol Med 14:303–311
33. Cardatoli E, Dotti MT, Hayek G, Zappella M, Federico A (1999) Studies on mitochondrial pathogenesis of Rett syndrome: ultrastructural data from skin and muscle biopsies and mutational analysis at mtDNA nucleotides 10463 and 2835. J Submicrosc Cytol Pathol 31:301–304
34. Gold WA, Williamson SL, Kaur S, Hargreaves IP, Land JM et al (2014) Mitochondrial dysfunction in the skeletal muscle of a mouse model of Rett syndrome (RTT): implications for the disease phenotype. Mitochondrion 15:10–17
35. Derecki NC, Privman E, Kipnis J (2010) Rett syndrome and other autism spectrum disorders-brain diseases of immune malfunction? Mol Psychiatry 15:355–363 **Review**
36. Jiang S, Li C, McRae G, Lykken E, Sevilla J et al (2014) MeCP2 reinforces STAT3 signaling and the generation of effector CD4+ T cells by promoting miR-124-mediated suppression of SOCS5. Sci Signal 7(316):ra25
37. Lee B, Cao R, Choi YS, Cho HY, Rhee AD et al (2009) The CREB/CRE transcriptional pathway: protection against oxidative stress-mediated neuronal cell death. J Neurochem 108:1251–1265
38. Pereira LO, Nabinger PM, Strapasson AC, Nardin P, Gonçalves CA et al (2009) Long-term effects of environmental stimulation following hypoxia–ischemia on the oxidative state and BDNF levels in rat hippocampus and frontal cortex. Brain Res 1247:188–195
39. Minetti M, Leto TH, Malorni W (2008) Radical generation and alterations of erythrocyte integrity as bioindicators of diagnostic or prognostic value in COPD? Antioxid Redox Signal 10:829–836
40. Rossi V, Leoncini S, Signorini C, Buonocore G, Paffetti P et al (2006) Oxidative stress and autologous immunoglobulin G binding to band 3 dimers in newborn erythrocytes. Free Radic Biol Med 40:907–915
41. Sierra C, Vilaseca MA, Brandi N, Artuch R, Mira A et al (2001) Oxidative stress in Rett syndrome. Brain Dev 1(Suppl):S236–S239
42. Kerr AM (1992) A review of the respiratory disorder in the Rett syndrome. Brain Dev 14(Suppl):S43–S45
43. Julu PO, Kerr AM, Apartopoulos F, Al-Rawas S, Engerström IW et al (2001) Characterization of breathing and associated central autonomic dysfunction in the Rett disorder. Arch Dis Child 85:29–37
44. De Felice C, Rossi M, Leoncini S, Chisci G, Signorini C et al (2014) Inflammatory lung disease in Rett syndrome. Mediators Inflamm 2014:560120
45. Ciccoli L, Signorini C, Alessandrini C, Ferrali M, Comporti M (1994) Iron release, lipid peroxidation, and morphological alterations of erythrocytes exposed to acrolein and phenylhydrazine. Exp Mol Pathol 60:108–118
46. Bobrowska-Hagerstrand M, Hagerstrand H, Iglic A (1998) Membrane skeleton and red blood cell vesiculation at low pH. Biochim Biophys Acta 1371:123–128
47. Vandegriff KD, Olson JS (1984) Morphological and physiological factors affecting oxygen uptake and release by red blood cells. J Biol Chem 259:12619–12627
48. Ciaccio C, Coletta A, De Sanctis G, Marini S, Coletta M (2008) Cooperativity and allostery in haemoglobin function. IUBMB Life 60:112–123
49. Agalakova NI, Gusev GP (2012) Fluoride induces oxidative stress and ATP depletion in the rat erythrocytes in vitro. Environ Toxicol Pharmacol 34:334–337
50. Rodríguez J, Di Pierro D, Gioia M, Monaco S, Delgado R et al (2006) Effects of a natural extract from Mangifera indica L, and its active compound, mangiferin, on energy state and lipid peroxidation of red blood cells. Biochim Biophys Acta 1760:1333–1342
51. Benesch RE, Benesch R, Kwong S, McCord JM (1986) Binding of diphosphoglycerate and ATP to oxyhemoglobin dimmers. J Mol Biol 190:481–485
52. Cortelazzo A, De Felice C, Guerranti R, Leoncini R, Barducci A et al (2016) Erythrocyte cytoskeletal-plasma membrane protein network in Rett syndrome: effects of ω-3 polyunsaturated fatty acids. Curr Proteomics 12:217–226
53. Huang TW, Kochukov MY, Ward CS, Merritt J, Thomas K et al (2016) Progressive changes in a distributed neural circuit underlie breathing abnormalities in mice lacking MeCP2. J Neurosci 36:5572–5586
54. Signorini C, De Felice C, Leoncini S, Durand T, Galano JM et al (2014) Altered erythrocyte membrane fatty acid profile in typical Rett syndrome: effects of omega-3 polyunsaturated fatty acid supplementation. Prostaglandins Leukot Essent Fatty Acids 91:183–193
55. Chakraborty S, Balakotaiah V, Bidani A (2004) Diffusing capacity reexamined: relative roles of diffusion and chemical reaction in red cell uptake of O2, CO, CO2, and NO. J Appl Physiol 97:2284–2302
56. Forster RE, Fowler WS, Bates DV (1954) Considerations on the uptake of carbon monoxide by the lungs. J Clin Invest. 33:1128–1134